How neural network structure alters the brain's self-organized criticality

Yoshiki A. Sugimoto[1], Hiroshi Yadohisa[1], Masato S. Abe[2,3,4,*]

1 Graduate School of Culture and Information Science, Doshisha University, Kyotanabe, Kyoto, Japan
2 Faculty of Culture and Information Science, Doshisha University, Kyotanabe, Kyoto, Japan
3 Center for Advanced Intelligence Project, RIKEN, Chuo-ku, Tokyo, Japan
4 Center for Brain Science BTCC TOYOTA Collaboration Center, RIKEN, Wako, Saitama, Japan

***maabe@mail.doshisha.ac.jp**

Abstract

In recent years, the "brain critical hypothesis" has been proposed in the fields of complex systems science and statistical physics, suggesting that the brain acquires functions such as information processing capabilities near the critical point, which lies at the boundary between disorder and order. As a mechanism for maintaining this critical state, a feedback system called "self-organized criticality (SOC)" has been proposed, where parameters related to brain function, such as synaptic plasticity, are maintained by internal rules without external adjustments. Additionally, the structure of neural networks plays an important role in information processing, with healthy neural networks being characterized by properties such as small-worldness, scale-freeness, and modularity. However, it has also been pointed out that these properties may be lacking in cases of neurological disorders. In this study, we used a mathematical model to investigate the possibility that differences in neural network structures could lead to brain dysfunction through SOC. As a result, it became clear that the synaptic plasticity conditions that maximize information processing capabilities vary depending on the network structure. Notably, when the network possesses only a scale-free structure, a phenomenon known as the Dragon king—associated with abnormal neural activity—was observed. These findings suggest that the maintenance of neural dynamics equilibrium differs depending on the structural characteristics of the neural network, and that in structures with hub nodes, such as scale-free networks, imbalances in neural dynamics may occur, potentially negatively impacting brain function.

Introduction

A number of empirical and theoretical studies have examined brain criticality hypothesis, which is derived from an idea in statistical physics and complex systems science [8, 56]. In brief, this hypothesis posits that neural networks operate near a critical point that is the boundary between disordered and ordered phases, and exhibit critical phenomena such as neuronal avalanches whose sizes follow a power-law distribution and long-range spatial or temporal correlations. Also, the properties stemmed from criticality can maximize some functions such as information processing capabilities and transmissions,

suggesting that a brain benefits from being critical [3, 10, 11, 23, 33, 68]. While much empirical evidence that brains exhibit critical properties has been accumulated [7, 9, 16, 17, 19, 20, 21, 22, 29, 35, 40, 42, 50, 57, 62, 67, 69, 73, 74, 76], a considerable number of studies reported that brain disorders are associated with non-critical (reviewed in [81]). For example, brain dynamics of individuals with neurological disorders, such as epilepsy and schizophrenia, did not show the signature of critlicaty such as long-range correlations [52, 58, 77]. Considering the benefits of criticality, it is natural that brain disorders may be influenced by loss of criticality. Thus, it is essential to elucidate how the deviations from critical states occur for understanding, predicticting, and controling brain disorders.

For the brain to be critical, the parameters underlying the brain system, such as synaptic strength, must be at or near the appropriate values, i.e., critical value. How are such parameters of the neural networks of (healthy) individuals tuned to be the value? It has been suggested that self-organized criticality (SOC) plays an important role for that [30]. SOC refers to a property of feedback systems homeostatically keeping a critical state based on its internal rules without external controls. An example of SOC in the brain is synaptic plasticity by which synaptic strength are adaptively tuned to a desireble state [7, 25, 33, 37, 42, 44, 45]. Previous studies showed that key parameters determining the system dynamics can hover around a critical point depending on parameters of SOC. This results in not a critical system perfectly tuned but a quasi-critical system.

Moreover, a peculiar phenomenon known as "Dragon Kings" may emerge through SOC [4, 5, 32, 64]. Dragon Kings refer to phenomena where a part of the distribution has a disproportionately large scale, deviating from the power-law distribution [1, 38, 41, 53, 60, 71, 72]. Dragon Kings have been observed in various systems, including financial markets, earthquakes, and weather phenomena [70]. In the brain, they are suggested to be associated with dysfunctions in neural activity, such as epilepsy [55]. Such abnormal neural activities may be the result of a breakdown in the self-organizing mechanisms that maintain the critical state. For instance, it has been reported through numerical simulations of spiking neural networks that rapid fluctuations in synaptic strength can lead to the emergence of Dragon Kings in the distribution of neuronal firing [32]. These results indicate that paramters of SOC impact system's dynamics and functional benefit.

While experimental evidence suggests that healthy neural networks may possess three key network structures: small-worldness, modularity, and scale-freeness [24], in neural networks associated with certain health issues, one or more of these properties are often found to be lacking. Although these facts indicate that network structures have important roles for information proccesing, how properties of networks contribute brain functions related to information processing remains insufficiently explored. One possible direction is to explore the relationship between brain criticality and network structures. Previous numerical studies show how the critical point changes depending on the structure of the neural network [15, 32, 59]. However, the way in which network structure affects the characteristics of SOC is not fully understood.

In the present study, we numerically investigated how network structures alter self-organiazed criticality. It has been suggested that neurological disorders such as epilepsy are associated with deviations of parameters related to brain function, such as synaptic strength, from the critical point. However, the mechanisms underlying this association are not yet fully understood. Previous studies have reported that neural networks in individuals with neurological disorders exhibit distinct structural features compared to healthy neural networks. Therefore, this study aims to test the hypothesis that differences in the structure of neural networks from a healthy state contribute to the onset of neurological disorders.

Materials and Methods

Modeling of Brain Systems.

To model brain systems, we utilize the Leaky Integrate-and-Fire (LIF) model [32, 59]. This model mathematically represents the firing phenomenon in which a neuron generates an electrical signal when its membrane potential exceeds a certain threshold, and transmits it to other connected neurons. Experimentally, neurons in the cerebral cortex have been observed to exhibit consistent responses to time-dependent inputs, with minimal variability in responses across trials when the same stimulus is repeated [12, 43]. In order to account for the subtle stochastic fluctuations in neuronal activity observed experimentally, this study adopts a probabilistic LIF model. Let N denote the number of neurons, and let X_i represent the firing of neuron i, where $X_i = 1$ indicates firing, and $X_i = 0$ indicates no firing. If neuron i fires at time t, then its membrane potential at time $t+1$ is set to $V_i[t+1] = 0$. When there is a connection from neuron j to neuron i, let neuron j be the presynaptic cell and neuron i the postsynaptic cell. The synaptic strength from neuron i to neuron j is denoted as W_{ij}, and the reverse connection is set as $W_{ji} = 0$. If there is no connection between neurons i and j, both W_{ij} and W_{ji} are set to 0. The time evolution of the membrane potential V_i is following:

$$V_i[t+1] = \mu_i V_i[t] + I_i[t] + \frac{1}{k_i}\sum_{j=1}^{N} W_{ij} X_j[t]. \tag{1}$$

Here, μ_i, $I_i[t]$, and k_i represent the leak parameter, external input at time t, and the number of synaptic connections of the postsynaptic neuron i, respectively.

The firing probability $\Phi(\cdot)$ of the postsynaptic neuron i is determined by its membrane potential V_i. Specifically, the probability becomes positive when V_i exceeds the threshold θ_i, and the larger the value of V_i, the higher the firing probability $\Phi(V_i[t])$. On the other hand, even when the membrane potential V_i does not exceed the threshold θ_i, neuron i may still fire spontaneously with a small probability, denoted as p_{spont}. This relationship is expressed as follows:

$$P\left(X_i[t] = 1 \mid V_i[t]\right) \equiv \begin{cases} \Phi\left(V_i[t]\right) & \text{if } V_i[t] - \theta_i > 0, \\ p_{\text{spont}} & \text{otherwise,} \end{cases} \tag{2}$$

$$\Phi\left(V_i[t]\right) = \frac{\Gamma_i\left(V_i[t] - \theta_i\right)}{1 + \Gamma_i\left(V_i[t] - \theta_i\right)} \Theta\left(V_i[t] - \theta_i\right), \tag{3}$$

$$\Theta\left(V_i[t] - \theta_i\right) = \begin{cases} 1 & \text{if } V_i[t] - \theta_i > 0, \\ 0 & \text{otherwise.} \end{cases} \tag{4}$$

In Eq. (3), Γ_i represents the gain parameter of the postsynaptic neuron i (with $\Gamma_i > 0.0$). Consequently, when the membrane potential V_i of the postsynaptic neuron exceeds the threshold value θ_i ($V_i > \theta_i$), the firing probability of the postsynaptic neuron i is determined by an increasing function of the gain parameter Γ_i and the difference between the membrane potential V_i and the threshold θ_i. In this study, unless otherwise specified, the following parameters are used: $N = 10000$, $\mu_i = 0.0$, $I_i[t] = 0.0$, $p_{\text{spont}} = 0.0001$, $\Gamma_i = 0.8$, and $\theta_i = 0.0$.

Derivation from the Critical Value.

We identify the critical value W_c of parameters that control brain dynamics, such as synaptic strength W_{ij}. To do so, we determine the parameter values that position the

brain state near the boundary between the disordered and ordered phases. To quantify the macroscopic state of the brain, we define the average firing rate $\rho[t]$ of neurons at time t as shown in the following equation:

$$\rho[t] \equiv \frac{1}{N} \sum_{i=1}^{N} X_i[t]. \tag{5}$$

Additionally, the average firing rate ρ of neurons over the time window from $t_t \sim t_f$ is defined by the following equation:

$$\rho \equiv \frac{1}{t_f - t_t + 1} \sum_{t=t_t}^{t_f} \rho[t]. \tag{6}$$

Based on the average firing rate ρ over the time window calculated from Eqs. (5) and (6), we identify the critical value W_c. Let W_c be the point which produces the maximum slope of a function $\rho(W)$. In the calculation, W_c was numerically examined in increments of 0.01 from 0 to 3.

The results of the critical values for each network structure are provided in the Supporting Information.

Mathematical Model for Self-Organized Criticality.

For SOC, various mathematical models have been proposed in previous studies [34]. Among these, we consider a model in which the synaptic strength W_{ij} fluctuates over time according to increasing and decreasing only when presynaptic neuron j is connected to postsynaptic neuron i. The time evolution of W_{ij} is described by

$$W_{ij}[t+1] = W_{ij}[t] + \frac{1}{\tau} - uW_{ij}[t]X_j[t]. \tag{7}$$

Here, τ is the time constant that determines how quickly the synaptic strength W_{ij} increases, and $u(0 < u < 1)$ is the synaptic depression coefficient. The synaptic strength W_{ij} for the connection from presynaptic neuron j to postsynaptic neuron i increases by a fixed amount at each time step but decreases when the postsynaptic neuron i fires. This mathematical model assumes synaptic plasticity and provides a simplified model for reproducing SOC. The initial value of the synaptic strength $W_{ij}[0]$ is set to the critical value W_c, and numerical analysis is performed.

Deviation Index from the Critical Value of Synaptic Strength.

As an indicator of how much the average synaptic strength $W[t]$ of the entire network at time t deviates from the critical value W_c, we calculate the Mean Absolute Error (MAE) according to Eqs. (8) and (9). Specifically, we compute the average of the absolute difference between $W[t]$ and the critical value W_c over the period from $t_a = 10^4$ to $t_b = 10^5$. The value $W[t]$ is the average synaptic strength of the entire network at time t, and it is calculated only for the connected node pairs $(i, j) \in E$. In other words, unconnected parts where $W_{ji} = 0$ are not included in the calculation. In this way, we analyze the variation in synaptic strength across the entire network.

$$MAE = \frac{1}{t_b - t_a + 1} \sum_{t=t_a}^{t_b} |W[t] - W_c| \,, \tag{8}$$

$$W[t] = \frac{1}{|E|} \sum_{(i,j)\in E} W_{ji}[t]. \tag{9}$$

Construction of Neural Networks.

To construct a network that exhibits small-world properties, scale-free characteristics, and modularity, we use the Watts-Strogatz (WS) model [75], the Barabási-Albert (BA) model [6], and the Stochastic Block (SB) model [27]. In order to investigate the impact of network structure on SOC, we generate five types of network structures: a regular network, a small-world network, a scale-free network, a modular network, and a random network constructed from the Erdős–Rényi (ER) model [18], with the number of neurons and synaptic connections kept consistent. Numerical analyses are conducted based on the LIF model. Details on the construction of the modular network are provided in the Supporting Information. Unless otherwise specified, we construct networks with an average degree of 8 in this study.

Classification of Neural Network Dynamics.

To understand the synaptic plasticity conditions under which neuronal avalanches occur, we classify the state of the neural network using the firing distribution based on the total number of neurons that fired in a cascade (Complementary Cumulative Distribution Function; CCDF). When the neural network reaches a critical state, cascades of varying sizes occur, and the CCDF follows a power law. On the other hand, when large-scale neuronal firings occur frequently, resulting in a deviation of the CCDF above the power law, a "Dragon king" phenomenon can occur [70]. One method to determine whether the Dragon king phenomenon is present is to test whether the distribution statistically matches a power law [28, 61]. Furthermore, studies investigating how Dragon kings arise in SOC have also employed statistical hypothesis testing [49]. However, in studies such as this one, which consider neural networks, the CCDF may not always follow a typical power law. Since no methods have been proposed to address such cases, we do not adopt the statistical hypothesis testing methods used in previous studies. Therefore, in this study, to understand the synaptic plasticity conditions under which neuronal avalanches occur, we classify firing states based on the CCDF of the total number of neurons involved in cascading firings into four categories: "Dragon king" (deviations from the power law due to frequent large-scale cascading firings), "Subcritical" (insufficient firing), "Critical" (a critical state following the power law), and "Supercritical" (large-scale cascading firings).

In the course of sufficient numerical analysis, depending on the values of the two parameters τ and u related to synaptic plasticity in Eq. (7), neurons may continue to fire in cascades over an extended period, resulting in fewer data points representing the number of neurons involved in the cascading firings. In this study, if the data points predominantly reflect only large-scale cascading firings, the state is classified as "Supercritical". If there are sufficient data points, the remaining states are classified into the other three categories. To prevent dependency on the initial state, we discard the first five data points and construct the CCDF. At this point, if the number of cascading firings is insufficient (less than $10^2.5$), the state is classified as "Subcritical". If the number of cascading firings is sufficient, the state is classified as either "Dragon king" or "Critical". To determine this, the distribution is fitted to a truncated power

law, and the classification is based on whether there is a deviation from the fitted distribution. For details on how the CCDF is fitted to a truncated power law, please refer to the Supporting Information. The reason for using a truncated power law instead of a power law is to account for the cutoff that may be observed due to the finite size of the network. If large-scale neuronal firings of more than 10^2 neurons occur with a frequency of less than 10^{-2}, and the CCDF deviates by a factor of 1.1 from the cumulative frequency of the truncated power law, the state is classified as "Dragon king." The CCDFs categorized into the four types using this method are provided in the Supporting Information.

Results

179

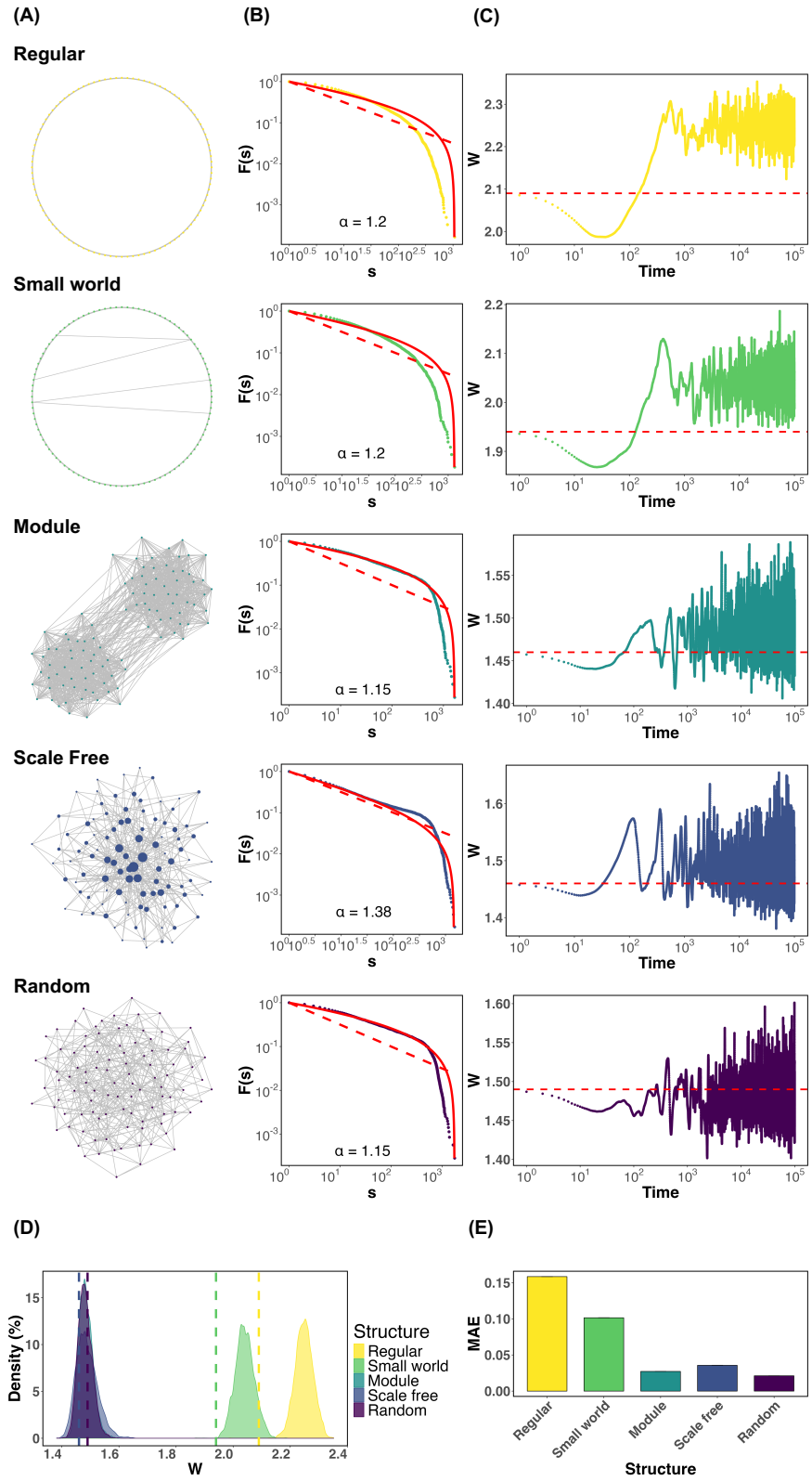
(A)
(B)
(C)
Regular
Small world
Module
Scale Free
Random
F(s)
s
α = 1.2
α = 1.2
α = 1.15
α = 1.38
α = 1.15
W
Time
(D)
(E)
Density (%)
W
Structure
Regular
Small world
Module
Scale free
Random
MAE
Structure

Figure 1. Firing distribution of neurons and time evolution of the average synaptic strength W for each network structure, assuming synaptic plasticity with $\tau = 600$ and $u = 0.1$. (A) Visualization of networks. All networks are drawn with $N = 100$ nodes and $m = 400$ edges for display purposes. In the scale-free network, the nodes are drawn larger in proportion to their degree. **(B)** CCDF based on the total number of neurons that fired in cascades. s represents the number of neurons that fired in a cascade. The red solid line represents the result of fitting the distribution to a truncated power law. α is the power-law exponent. The red dashed line indicates the theoretical value $\alpha = 1.5$, derived analytically without considering the network structure. **(C)** Visualization of the time evolution of the average synaptic strength W. The red dashed line represents the critical value W_c. **(D)** Probability Density Function (PDF) of the average synaptic strength W. The dashed lines indicate the critical values W_c for each network. **(E)** The MAE, an indicator of how much the average synaptic strength W deviates from the critical value W_c, was calculated for each network according to Eqs. (8) and (9).

First, based on the neural network structure and the parameters $\tau = 600$ and $u = 0.1$ of the equation for synaptic plasticity (7), we present graphs showing the conditions for the occurrence of the critical state and the deviation of the average synaptic strength W from the critical value W_c. These graphs include the CCDF based on the total number of neurons that fired in a cascade (Fig. 1A), the time series of the average synaptic strength W (Fig. 1B), the Probability Density Function (PDF) of the average synaptic strength W for each network structure (Fig. 1C), and the MAE values for each network structure (Fig. 1D). The CCDF follows a truncated power law, except in the case of the scale-free network (Fig. 1B). In the scale-free network, a Dragon king phenomenon occurs, where the distribution deviates from the power law (Fig. 1B; Scale free). It should be noted that the power law is not exclusive to the critical state, so we verify that several power laws arise near the critical point W_c, such as the number of neurons firing in a cascade, the duration of firing, and the relationship between these two, all of which follow scaling laws [65, 66]. These results are presented in the Supporting Information (Fig. S5). The results show that the data points for the number of neurons firing in cascades and the duration of firing align reasonably well with the slope $(\alpha–1)/(\beta–1)$ (Fig. S5C). However, the alignment of the slope $(\alpha–1)/(\beta–1)$ in the scale-free network, which exhibits a Dragon king phenomenon, remains a subject for debate. Based on these findings, it is considered that a critical state is realized under the synaptic plasticity conditions of $\tau = 600$ and $u = 0.1$, except for the scale-free network. Additionally, it was revealed that the average synaptic strength W deviates from the critical value W_c, depending on the network structure (Fig. 1C, D, E). In both the regular and small-world networks, the average synaptic strength W deviates above the critical value W_c(Fig. 1C, D; Regular, Small world), and the MAE shows large values (Fig. 1E). In contrast, for the modular, scale-free, and random networks, the average synaptic strength W does not deviate significantly from the critical value W_c (Fig. 1C, D; Module, Scale free, Random), and the MAE exhibits similar values (Fig. 1E). From these results, it was found that, under the synaptic plasticity conditions of $\tau = 600$ and $u = 0.1$, a critical state was achieved in all network structures except for the scale-free network, and regardless of the results, the average synaptic strength W deviated from the critical value W_c in the regular and small-world networks.

Next, based on the neural network structure and the parameters τ, u for synaptic plasticity in the Eq. (7), we show the conditions for the occurrence of the critical state and the deviation of the average synaptic strength W from the critical value W_c (Fig. 2). In the scale-free network, compared to other networks, there are many

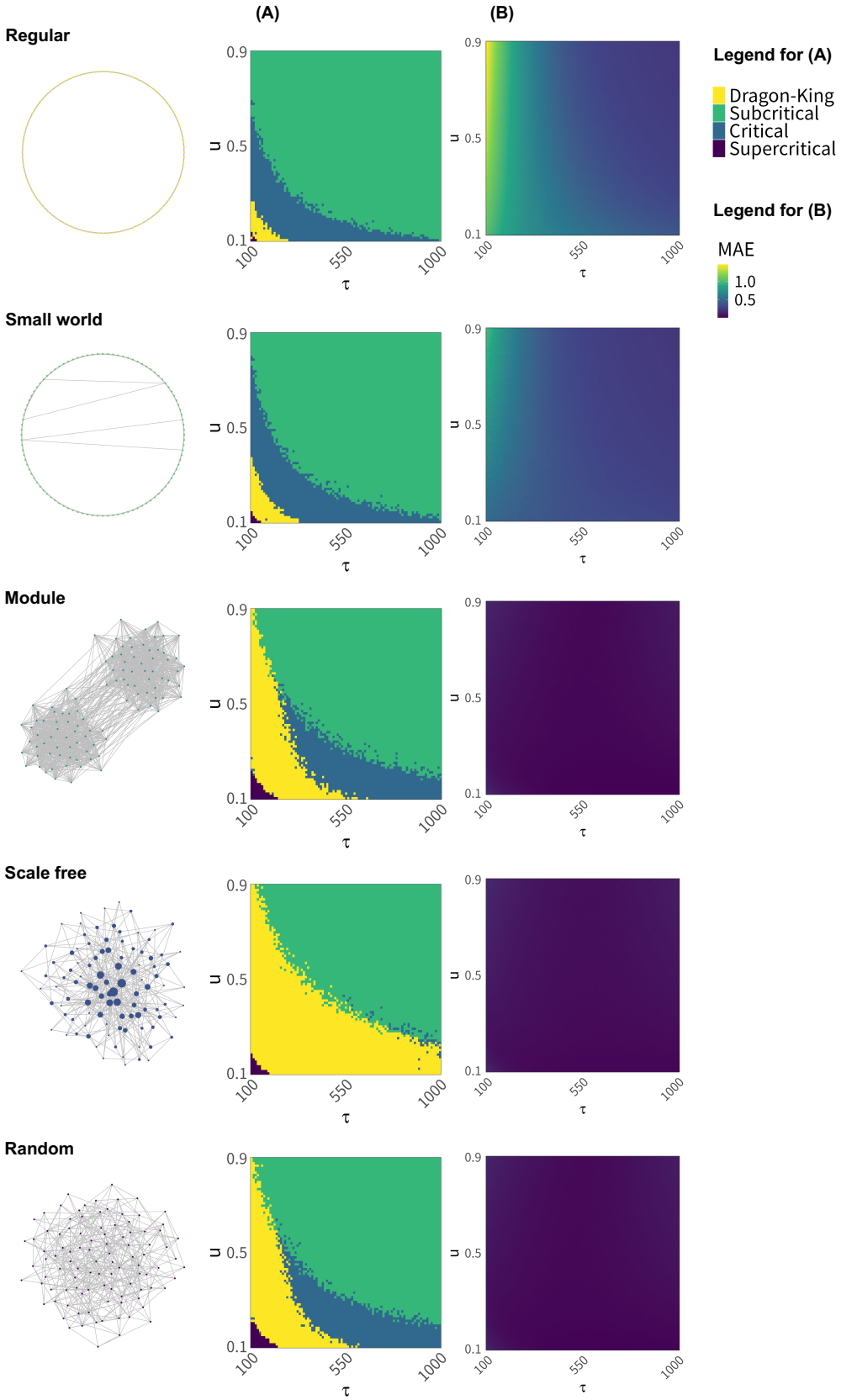
(A)
(B)
Regular
Small world
Module
Scale free
Random
u
τ
0.9
0.5
0.1
100
550
1000
Legend for (A)
Dragon-King
Subcritical
Critical
Supercritical
Legend for (B)
MAE
1.0
0.5

Figure 2. The state of the neural network and the deviation of the average synaptic strength W from the critical value W_c, assuming various synaptic plasticity conditions and different neural network structures. The state of the neural network and the deviation of the average synaptic strength W from the critical value W_c were compared across different network structures when various synaptic plasticity conditions were assumed within the range of $100 \leq \tau \leq 1000$ and $0.1 \leq u \leq 0.9$ in Eq. (7). **(A)** For each value of the time constant τ and synaptic depression coefficient u, the state of the neural network is classified as "Dragon king", "Subcritical", "Critical", or "Supercritical", and the results are indicated by color. **(B)** For each value of the time constant τ and synaptic depression coefficient u, the degree of deviation of the average synaptic strength W from the critical value W_c is calculated using the MAE indicator according to Eqs. (8) and (9).

conditions of synaptic plasticity that lead to the occurrence of the Dragon king phenomenon, and it was revealed that the critical state is not achieved under most synaptic plasticity conditions (Fig. 2A; Scale free). In regular and small-world networks, the critical state is achieved when the time constant τ is small and the synaptic depression coefficient u is relatively large, or when τ is large and u is small (Fig. 2A; Regular, Small world). In modular and random networks, the critical state is realized when τ is large and u is small (Fig. 2A; Module, Random). The situations where the average synaptic strength W deviates from the critical value W_c also differ depending on the network structure, with notable deviations in the regular and small-world networks (Fig. 2B; Regular, Small world). Additionally, changing the average degree of the network or the number of modules B in the modular network did not alter the conditions for the occurrence of the critical state (Fig. S7, S8). On the other hand, altering the leak parameter in the LIF model significantly changed the conditions for the occurrence of the critical state (Fig. S6). These results suggest that the synaptic plasticity conditions required to maintain the critical state vary depending on the structural characteristics of the network and the state of neural activity, and that there is a weak relationship between maintaining the critical state and the deviation of the average synaptic strength W from the critical value W_c.

From the results so far, it has become clear that in regular and small-world networks, the average synaptic strength W deviates from the critical value W_c (Fig. 3B; Regular, Small world). But why does this happen? To clarify the reason, we focus on a specific point in time and examine the individual synaptic strengths. The values of synaptic strength $W_{ij}[10^4]$ from neuron j to neuron i at time $t = 10^4$ are shown as a histogram (Fig. 3A). The results reveal that, compared to the random network, the distributions of synaptic strength $W_{ij}[10^4]$ in the regular and small-world networks have wider tails and higher values of synaptic strength $W_{ij}[10^4]$. Furthermore, to investigate why the individual synaptic strengths differ depending on the network structure, we visualized how neurons fire in the network using a raster plot (Fig. 3B). The results show that in regular and random networks, neurons fire locally within the network. Based on these findings, it is considered that in regular and small-world networks, because neurons fire locally, synaptic strength decreases in some areas, but most of the network remains inactive. As a result, the average synaptic strength across the entire network increases and deviates from the critical value.

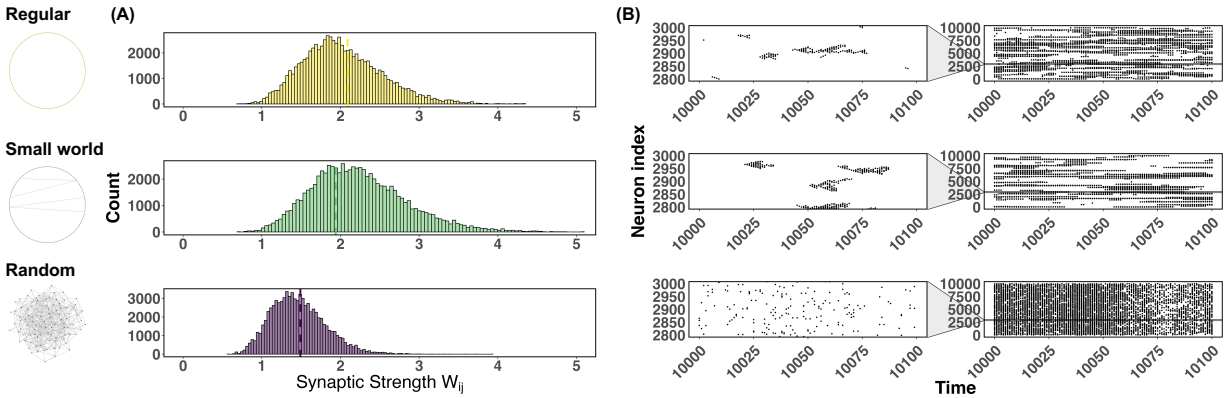

Figure 3. Synaptic strength W_{ij} and raster plot for the regular, small-world, and random networks at time $t = 10^4$. (A) Histogram of the synaptic strength W_{ij} from neuron j to neuron i in the regular, small-world, and random networks at time $t = 10^4$. The dashed lines represent the critical value W_c for each network. **(B)** Raster plot showing the firing activity of neurons in the regular, small-world, and random networks. Black dots indicate neurons that fired, while white areas represent non-firing neurons.

Discussion

In this study, we used a mathematical model to examine how differences in neural network structures influence the realization of SOC through synaptic plasticity and how they may cause critical states or not in brain systems. First, it became clear that the conditions for achieving a critical state vary depending on the network structure. Additionally, under certain network structures and synaptic plasticity conditions, the Dragon king phenomenon—associated with neuronal dysfunction—was observed, particularly in the scale-free network. This result suggests that flexibly adapting synaptic plasticity according to the structure of the neural network can contribute to maximizing information processing capabilities. Previous studies suggested that scale-free networks might be efficient for computations [24]. However, our study revealed that under SOC-inducing conditions, the structural characteristics of scale-free networks may lead to dysfunctions in neural activity.

To better understand the dysfunction of neural activity, such as epilepsy, various approaches are used beyond just the brain criticality hypothesis. From a physiological perspective, it has been reported that epilepsy is caused by excessive activation of glutamatergic neurons and a lack of proper inhibition by GABAergic neurons, which is associated with imbalances in neural circuits [80]. Furthermore, disturbances in ion balance within neural networks have been pointed out as contributing to the complexity of epileptic seizures through changes in voltage-gated sodium and potassium channels, as well as the formation of various ion channels [39, 49]. In theoretical neuroscience, Dragon king phenomena associated with epilepsy have been reported to occur alongside major shifts from supercritical to critical states [49], suggesting that this impacts imbalances in neural dynamics. Thus, the mechanisms of dysfunction in neural activity, such as epilepsy, are becoming clearer through various approaches, but previous studies have emphasized that the balance and dynamics of neural circuits play a crucial role. Based on previous findings and the results of this study, we propose that the conditions for maintaining balanced neural dynamics differ depending on the structural characteristics of the neural network. In networks with structural characteristics like those in scale-free networks that have hub nodes, imbalances in neural dynamics often arise, which can negatively affect brain function.

Additionally, this study revealed that there is no direct correlation between average synaptic strength behavior and the state of the neural network. For instance, while the synaptic strength may deviate from the critical value, the neural network can still achieve a critical state. Conversely, while the average synaptic strength may behave near the critical value, abnormal phenomena like Dragon king can occur. This result suggests that it is not easy to determine the state of the neural network based solely on the behavior of average synaptic strength. Previous studies analyzing empirical data have pointed out a correlation between parameters controlling neural dynamics deviating above the critical value and epilepsy [2, 13, 14, 26, 36, 46, 48, 51, 52, 54, 55, 58, 63, 77, 78, 79, 81] or prolonged sleep deprivation [47, 81]. Based on previous studies and the results of this study, we suggest that in networks characterized by local connections deviating from the critical value, neural plasticity conditions may maximize information processing capabilities, while also contributing to conditions like epilepsy or prolonged sleep deprivation.

Finally, we would like to conclude this paper by addressing important issues that will become relevant in the future in relation to this research. Beyond discussions about which neural network structures and synaptic plasticity conditions maximize information processing capabilities, it is essential to focus on behavior and embodiment, such as motor control and emotional expression, and to understand how neural network structures relate to these functions. If we can understand the mechanisms of behavior and embodiment from a brain perspective, we might better understand how brain-based disorders like motor dysfunctions associated with developmental disorders arise. From a medical perspective, predicting the state of the neural network based on neural dynamics, such as synaptic strength, is also an important area of applied research. Additionally, apart from the concept of neural activity, it will be important to explore how SOC reproducible by toy models, such as the sandpile model [5], aligns with SOC related to synaptic plasticity in the brain and whether toy models can reproduce neural dynamics. This will be crucial for understanding the relationship between SOC and the brain.

Supporting Information

Materials and Methods

Construction of Modular Networks.

The Stochastic Block (SB) model constructs a modular network by generating synaptic connections (edges) between neurons (nodes) within and between modules probabilistically. Therefore, depending on the edge generation probability, the number of synaptic connections can vary significantly. To compare with other networks such as regular networks, it is necessary to first determine the number of neurons and the expected number of synaptic connections, and then derive the edge generation probability to construct the modular network. In this study, synaptic connections within each module are generated with probability p_B, and synaptic connections between modules are generated with probability q_B. Let the number of modules be B, the number of neurons be N (where $N \bmod B = 0$), the total number of synaptic connections within all modules be m_p, the total number of synaptic connections between all modules be m_q (with $m_p : m_q = r : 1$), and the total number of synaptic connections in the entire network be m (where $m_p + m_q = m$). Based on this, we derive the synaptic connection probability p_B within each module and the synaptic connection probability q_B between modules.

First, the total number of synaptic connections within all modules m_p and the total number of synaptic connections between all modules m_q can be derived as:

$$m_p = \frac{1}{r+1}m, \quad m_q = \frac{r}{r+1}m. \tag{S1}$$

Next, let Π_p be the number of neuron pairs within modules, and Π_q be the number of neuron pairs between modules:

$$\Pi_p = \binom{B}{2}\left(\frac{N}{B}\right)^2 = \frac{B(B-1)}{2}\left(\frac{N}{B}\right)^2 = \frac{(B-1)N^2}{2B}, \tag{S2}$$

$$\Pi_q = B\binom{\frac{N}{B}}{2} = \frac{N^2}{2B} - \frac{N}{2}. \tag{S3}$$

From this, the synapse generation probability p_B within each module and the synapse generation probability q_B between modules can be derived as:

$$p_B = \frac{m_p}{\Pi_p} = \frac{\frac{1}{r+1}m}{\frac{(B-1)N^2}{2B}} = \frac{2Bm}{(r+1)(B-1)N^2}, \tag{S4}$$

$$q_B = \frac{m_q}{\Pi_q} = \frac{\frac{r}{r+1}m}{\frac{N^2}{2B} - \frac{N}{2}} = \frac{2Brm}{(r+1)\left(N^2 - BN\right)}. \tag{S5}$$

Fitting to a Truncated Power Law.

We explain the method for fitting the CCDF based on the total number of neurons firing in cascades and the duration of firing to a truncated power law. A truncated power law is a model suited for data constrained within a specific lower and upper bound. Here, we collectively refer to the data, such as the total number of neurons firing in cascades and the duration of firing, which are subject to fitting to a truncated power law, as D. For the observed data $D_1, D_2, \ldots, D_L$, the log-likelihood function is defined by the following Eq. (S6) [31]:

$$\mathcal{L}(e) = \sum_{l=1}^{L} \log\left(\frac{D_{\max}^e D_{\min}^e}{D_{\max}^e - D_{\min}^e} \times D_l^{-1-e}\right) \tag{S6}$$

In this equation, $D_{\min}$ represents the minimum value of the data, and $D_{\max}$ represents the maximum value of the data. The parameter e is the power-law exponent estimated from the data and is a critical parameter that determines the shape of the distribution. In the method of maximum likelihood estimation, the value of e that maximizes the log-likelihood function $\mathcal{L}(e)$ is sought. Specifically, by varying e and calculating the value of the likelihood function for the observed data $D_1, D_2, \ldots, D_L$, the value of e that maximizes the likelihood is estimated. This process determines the shape parameter e of the truncated power law that best fits the data. Using this method, we can estimate an appropriate distribution model for data such as the total number of neurons firing in cascades and the duration of firing.

Results

Critical Values for Each Network Structure.

The average firing rate ρ of neurons obtained from the average synaptic strength W_k is shown (Fig. S1 to S3). The results for the random network (Fig. S1 to S2; Random)

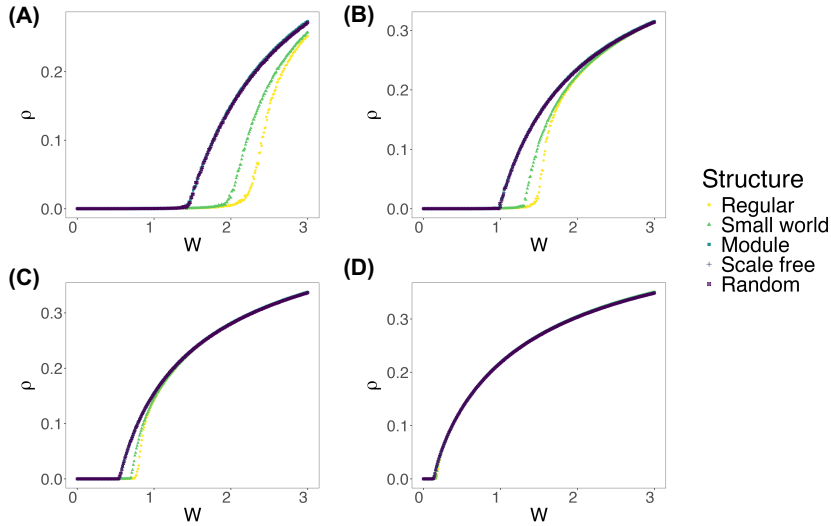

Figure S1. The relationship between the average synaptic strength W and the average firing rate ρ of neurons when varying the leak parameter μ in the LIF model. (A) $\mu = 0.0$. **(B)** $\mu = 0.3$. **(C)** $\mu = 0.6$. **(D)** $\mu = 0.9$.

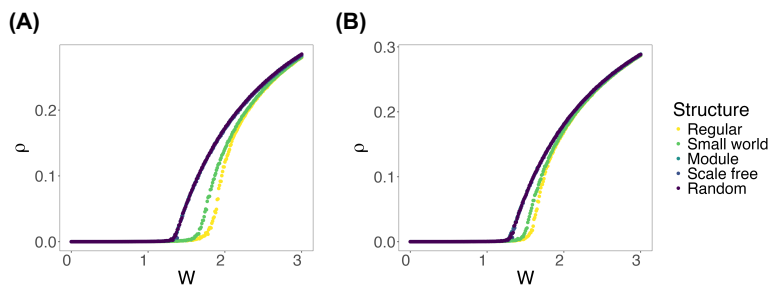

Figure S2. The relationship between the average synaptic strength W and the average firing rate ρ of neurons when varying the average degree in the neural network. The case with an average degree of 8 corresponds to Fig. S1A. **(A)** Case with an average degree of 16. **(B)** Case with an average degree of 32.

and the network with an increased number of synaptic connections (Fig. S2) are close to the mean-field approximation, resulting in values near $W_c = 1/\Gamma$ [59]. Moreover, the results when varying μ are consistent with previous studies [59]. Additionally, the results when varying the number of modules B did not significantly affect the numerical analysis and were similar to the random network scenario.

Classification Results of Neural Network States.

This figure illustrates under which conditions of synaptic plasticity the neural network reaches the states of "Dragon king," "Subcritical," "Critical," or "Supercritical" (Fig. S4). When the firing distribution deviates above the truncated power law, it is defined as a "Dragon king" (Fig. S4A). At this point, data points that slightly deviate from the truncated power law are not classified as "Dragon king" due to the threshold. In this study, data points that deviate more than 1.1 times from the truncated power law fitting result are classified as "Dragon king". When the maximum number of neurons

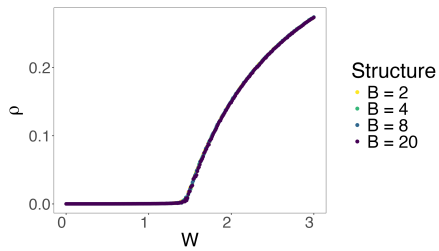

Figure S3. The relationship between the average synaptic strength W and the average firing rate ρ of neurons when varying the number of modules B in the neural network. The case with the number of modules $B = 2$ corresponds to Fig. S1A (Module).

firing in a cascade falls below the threshold (set to 10^2 in this study), the network is classified as "Subcritical", as not enough neurons fired in cascades (Fig. S4B). In the "Supercritical" case, there is only one data point because there was no time when neurons did not fire, resulting in large-scale cascading firings (Fig. S4D).

On the Scaling Laws Between Multiple Power Laws.

Near the critical value W_c, multiple power laws exist, not only for the number of neurons firing in cascades but also for the duration of the firing and the relationship between these two. A relationship called the "scaling law" holds between these different power exponents. Let α be the power exponent for the number of neurons firing in cascades (dependent variable), and β be the power exponent for the duration of the firing (dependent variable). Let γ represent the slope that explains the relationship between these two. In the critical state, the following equation holds: $(\alpha - 1)/(\beta - 1) = \gamma$. Numerical analysis using a mathematical model that assumes synaptic plasticity in various neural networks (Fig. S5) showed that, for all networks, the data points for the number of neurons firing in cascades and the duration of the firing roughly align with the slope $(\alpha - 1)/(\beta - 1) = \gamma$. Therefore, it can be considered that the scaling law is valid, and the neural network is in a critical state.

The State of Neural Networks When Varying the Leak Parameter in the LIF Model.

This figure illustrates how the state of the neural network changes when varying the Leak parameter μ in the LIF model (Fig. S6). The results show that the structure of the neural network changes significantly depending on the value of the leak parameter μ.

The State of Neural Networks When Varying the Average Degree.

This figure illustrates how the state of the neural network changes when varying the average degree (Fig. S7). The results reveal that the state of the neural network shows little change depending on the average degree.

The State of Neural Networks When Varying the Number of Modules

This figure illustrates how the state of the neural network changes when varying the number of modules B in a modular network (Fig. S8). The results show that the state of the neural network exhibits little change depending on the number of modules B.

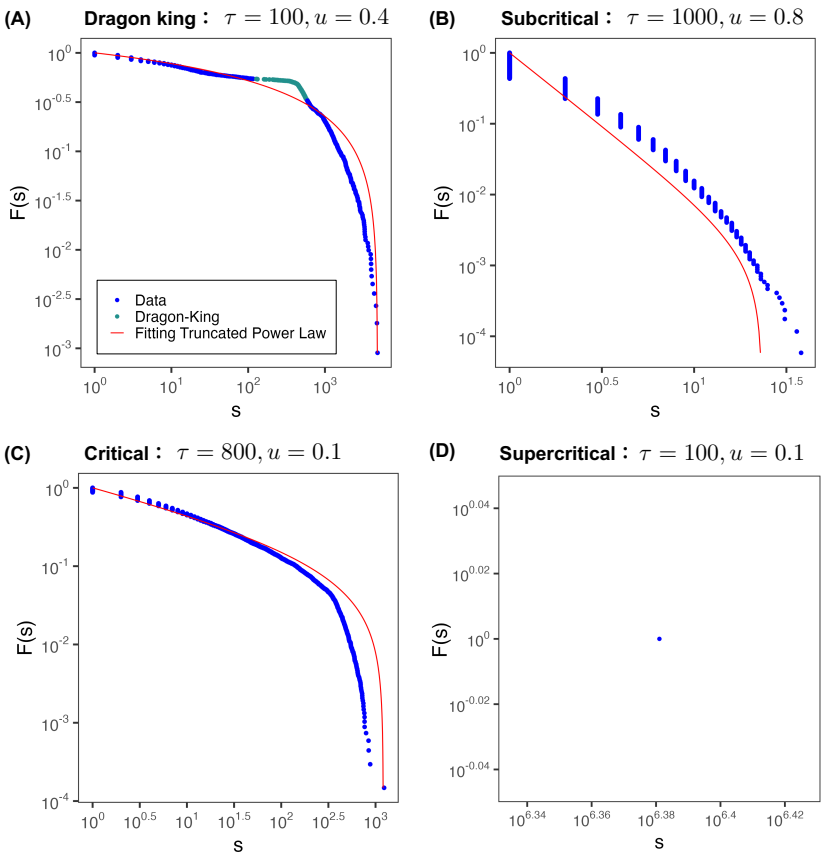

Figure S4. Classification results of neural network states. The figure shows the classification of the neuron firing distribution obtained from the numerical analysis of the synaptic plasticity model in Eq. (7) into "Dragon king," "Subcritical," "Critical," and "Supercritical". Blue dots represent data points, the red curve shows the fitting result from the truncated power law, and green dots represent data points classified as Dragon king. All results are from random networks. **(A)** Dragon king: $\tau = 100, u = 0.4$. **(B)** Subcritical: $\tau = 1000, u = 0.8$. **(C)** Critical: $\tau = 800, u = 0.1$. **(D)** Supercritical: $\tau = 100, u = 0.1$.

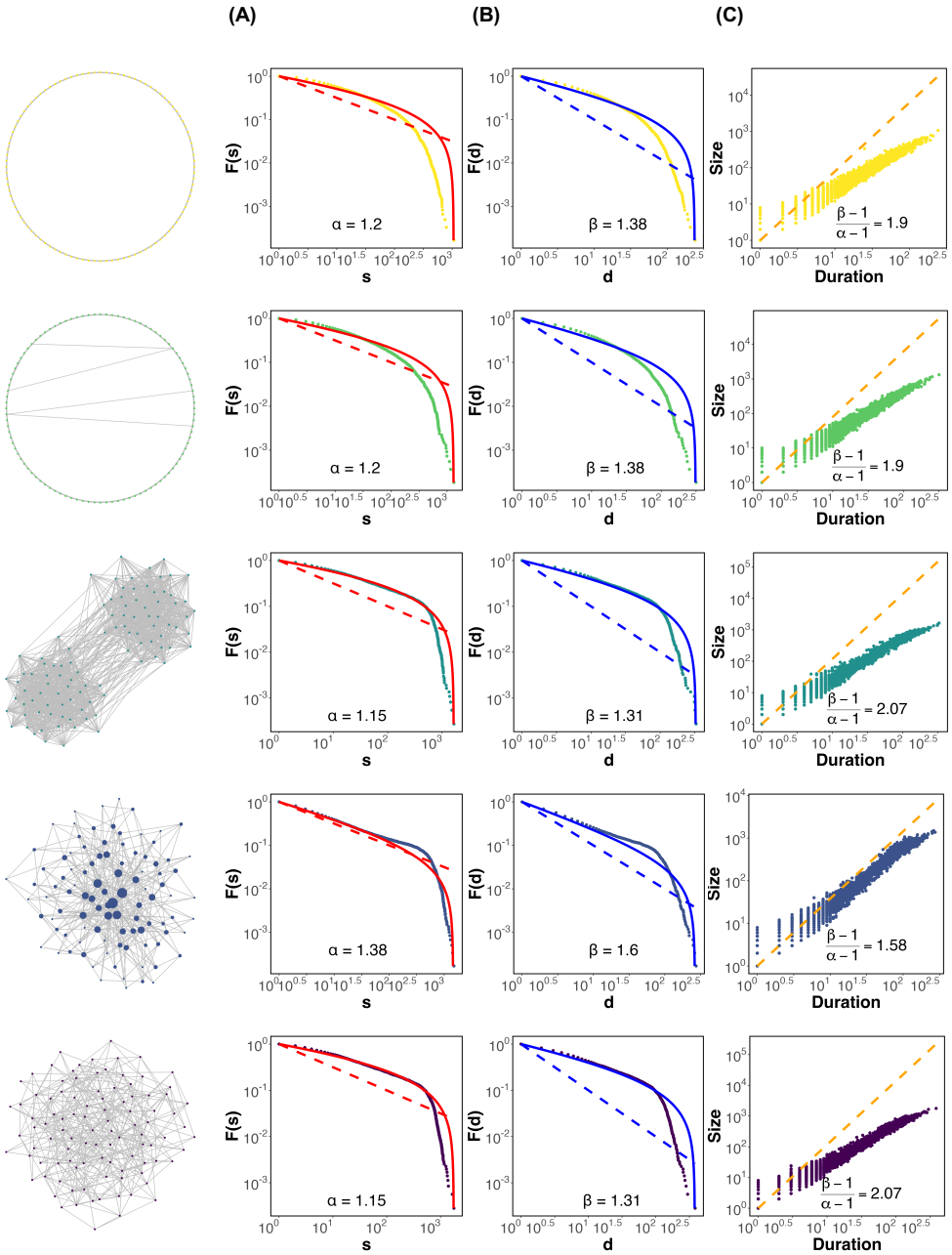

Figure S5. The number of neurons firing in cascades and the duration of firing, and the relationship between these two. By plotting the CCDF for the number of neurons firing in cascades, the CCDF for the duration of firing, and a scatter plot showing the relationship between these two for each network structure, the scaling laws between multiple power laws are verified. **(A)** CCDF based on the total number of neurons firing in cascades. This is the same as Fig. 1B. **(B)** CCDF based on the duration of cascaded firing. d represents the duration of cascaded firing. The blue solid line shows the fitting result to the truncated power law. β is the power-law exponent. The blue dashed line represents the theoretical value $\beta = 2.0$, derived analytically. **(C)** Scatter plot of the number of neurons firing in cascades and the duration of firing. The orange dashed line shows the slope $(\alpha–1)/(\beta–1) = \gamma$.

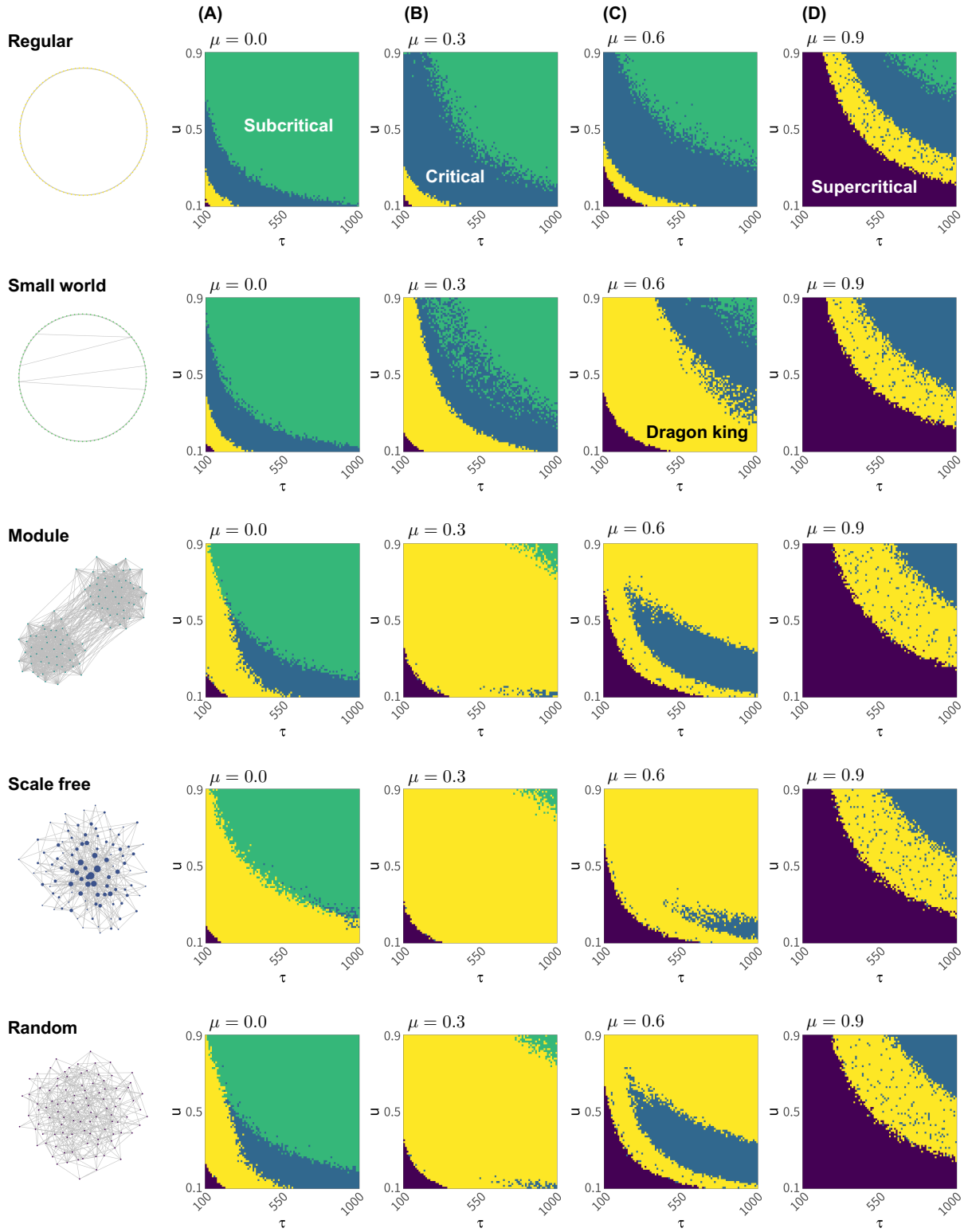

Figure S6. The state of the neural network when varying the leak parameter in the LIF model. Assuming synaptic plasticity within the range of $100 \leq \tau \leq 1000$ and $0.1 \leq u \leq 0.9$ in Eq. (7), numerical analysis was conducted to show under which synaptic plasticity conditions the critical state is realized, for each value of the leak parameter μ in the LIF model and for each network structure. The results for $\mu = 0.0$ are the same as Fig. 2A. **(A)** $\mu = 0.0$. **(B)** $\mu = 0.3$. **(C)** $\mu = 0.6$. **(D)** $\mu = 0.9$.

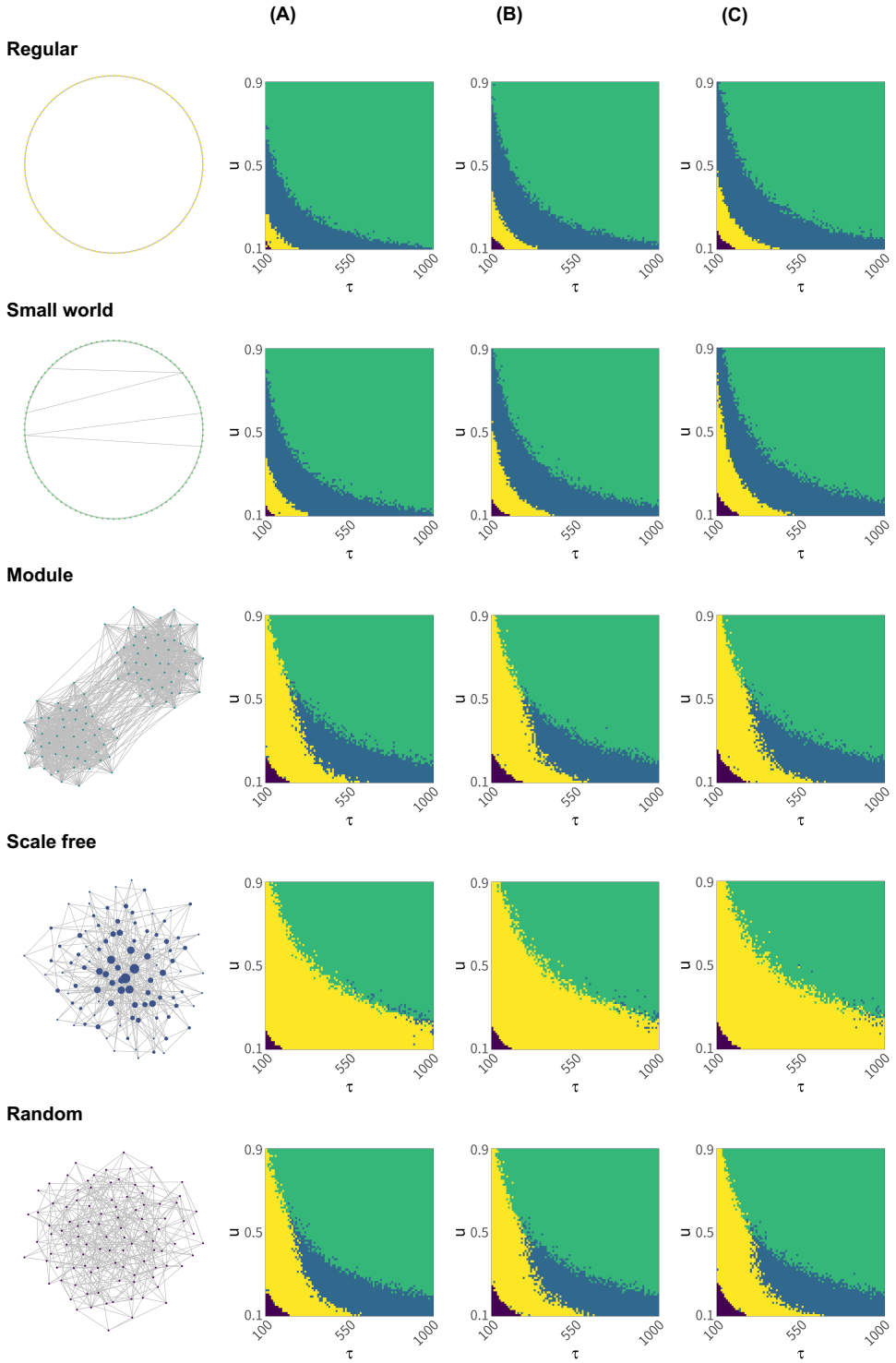

Figure S7. The state of the neural network when varying the average degree in the neural network. Assuming synaptic plasticity within the range of $100 \leq \tau \leq 1000$ and $0.1 \leq u \leq 0.9$ in Eq. (7), numerical analysis was conducted to show under which synaptic plasticity conditions the critical state is realized for neural networks with different average degrees. The results for an average degree of 8 are the same as Fig. 2A. **(A)** Average degree 8. **(B)** Average degree 16. **(C)** Average degree 32.

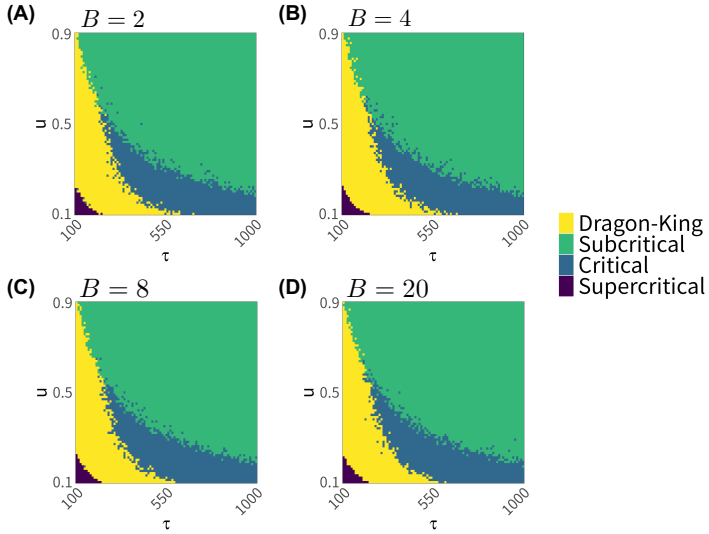

Figure S8. The state of the neural network when varying the number of modules B in the neural network. Assuming synaptic plasticity within the range of $100 \leq \tau \leq 1000$ and $0.1 \leq u \leq 0.9$ in Eq. (7), numerical analysis was conducted to show under which synaptic plasticity conditions the critical state is realized for neural networks with different numbers of modules B. The results for $B = 2$ are the same as Fig. 2A (Module). **(A)** $B = 2$. **(B)** $B = 4$. **(C)** $B = 8$. **(D)** $B = 20$.

Acknowledgments

This study was supported by JSPS KAKENHI Grant Number JP22K12235.

References

1. D. Amitrano. Variability in the power-law distributions of rupture events: How and why does b-value change. *The European Physical Journal Special Topics*, 205(1):199–215, 2012.

2. O. Arviv, M. Medvedovsky, L. Sheintuch, A. Goldstein, and O. Shriki. Deviations from critical dynamics in interictal epileptiform activity. *Journal of Neuroscience*, 36(48):12276–12292, 2016.

3. A.-E. Avramiea, A. Masood, H. D. Mansvelder, and K. Linkenkaer-Hansen. Long-range amplitude coupling is optimized for brain networks that function at criticality. *Journal of Neuroscience*, 42(11):2221–2233, 2022.

4. P. Bak. *How nature works: the science of self-organized criticality*. Springer Science & Business Media, 2013.

5. P. Bak, C. Tang, and K. Wiesenfeld. Self-organized criticality: An explanation of the 1/f noise. *Physical review letters*, 59(4):381, 1987.

6. A.-L. Barabási and R. Albert. Emergence of scaling in random networks. *science*, 286(5439):509–512, 1999.

7. J. M. Beggs and D. Plenz. Neuronal avalanches in neocortical circuits. *Journal of neuroscience*, 23(35):11167–11177, 2003.

8. J. M. Beggs and N. Timme. Being critical of criticality in the brain. *Frontiers in physiology*, 3:163, 2012.

9. T. Bellay, A. Klaus, S. Seshadri, and D. Plenz. Irregular spiking of pyramidal neurons organizes as scale-invariant neuronal avalanches in the awake state. *Elife*, 4:e07224, 2015.

10. N. Bertschinger and T. Natschläger. Real-time computation at the edge of chaos in recurrent neural networks. *Neural computation*, 16(7):1413–1436, 2004.

11. J. Boedecker, O. Obst, J. T. Lizier, N. M. Mayer, and M. Asada. Information processing in echo state networks at the edge of chaos. *Theory in Biosciences*, 131:205–213, 2012.

12. H. L. Bryant and J. P. Segundo. Spike initiation by transmembrane current: a white-noise analysis. *The Journal of physiology*, 260(2):279–314, 1976.

13. R. Cerf, E. H. E. Ouasdad, and P. Kahane. Criticality and synchrony of fluctuations in rhythmical brain activity: pretransitional effects in epileptic patients. *Biological cybernetics*, 90(4):239–255, 2004.

14. M. J. Cook, A. Varsavsky, D. Himes, K. Leyde, S. F. Berkovic, T. O'Brien, and I. Mareels. The dynamics of the epileptic brain reveal long-memory processes. *Frontiers in neurology*, 5:217, 2014.

15. A. A. Costa, L. Brochini, and O. Kinouchi. Self-organized supercriticality and oscillations in networks of stochastic spiking neurons. *Entropy*, 19(8):399, 2017.

16. A. Daffertshofer, R. Ton, M. L. Kringelbach, M. Woolrich, and G. Deco. Distinct criticality of phase and amplitude dynamics in the resting brain. *Neuroimage*, 180:442–447, 2018.

17. D. Dahmen, S. Grün, M. Diesmann, and M. Helias. Second type of criticality in the brain uncovers rich multiple-neuron dynamics. *Proceedings of the National Academy of Sciences*, 116(26):13051–13060, 2019.

18. P. ERDdS and A. R&wi. On random graphs i. *Publ. math. debrecen*, 6(290-297):18, 1959.

19. E. D. Fagerholm, R. Lorenz, G. Scott, M. Dinov, P. J. Hellyer, N. Mirzaei, C. Leeson, D. W. Carmichael, D. J. Sharp, W. L. Shew, et al. Cascades and cognitive state: focused attention incurs subcritical dynamics. *Journal of Neuroscience*, 35(11):4626–4634, 2015.

20. D. Fraiman, P. Balenzuela, J. Foss, and D. R. Chialvo. Ising-like dynamics in large-scale functional brain networks. *Physical Review E—Statistical, Nonlinear, and Soft Matter Physics*, 79(6):061922, 2009.

21. E. D. Gireesh and D. Plenz. Neuronal avalanches organize as nested theta-and beta/gamma-oscillations during development of cortical layer 2/3. *Proceedings of the National Academy of Sciences*, 105(21):7576–7581, 2008.

22. G. Hahn, A. Ponce-Alvarez, C. Monier, G. Benvenuti, A. Kumar, F. Chavane, G. Deco, and Y. Frégnac. Spontaneous cortical activity is transiently poised close to criticality. *PLoS computational biology*, 13(5):e1005543, 2017.

23. C. Haldeman and J. M. Beggs. Critical branching captures activity in living neural networks¡? format?¿ and maximizes the number of metastable states. *Physical review letters*, 94(5):058101, 2005.

24. K. Heiney, O. Huse Ramstad, V. Fiskum, N. Christiansen, A. Sandvig, S. Nichele, and I. Sandvig. Criticality, connectivity, and neural disorder: a multifaceted approach to neural computation. *Frontiers in computational neuroscience*, 15:611183, 2021.

25. J. Hesse and T. Gross. Self-organized criticality as a fundamental property of neural systems. *Frontiers in systems neuroscience*, 8:166, 2014.

26. J. P. Hobbs, J. L. Smith, and J. M. Beggs. Aberrant neuronal avalanches in cortical tissue removed from juvenile epilepsy patients. *Journal of Clinical Neurophysiology*, 27(6):380–386, 2010.

27. P. W. Holland, K. B. Laskey, and S. Leinhardt. Stochastic blockmodels: First steps. *Social networks*, 5(2):109–137, 1983.

28. J. Janczura and R. Weron. Black swans or dragon-kings? a simple test for deviations from the power law. *The European Physical Journal Special Topics*, 205(1):79–93, 2012.

29. M. Jannesari, A. Saeedi, M. Zare, S. Ortiz-Mantilla, D. Plenz, and A. A. Benasich. Stability of neuronal avalanches and long-range temporal correlations during the first year of life in human infants. *Brain Structure and Function*, 225:1169–1183, 2020.

30. H. J. Jensen. *Self-organized criticality: emergent complex behavior in physical and biological systems*, volume 10. Cambridge university press, 1998.

31. Y. Y. Kagan. Seismic moment distribution revisited: I. statistical results. *Geophysical Journal International*, 148(3):520–541, 2002.

32. O. Kinouchi, L. Brochini, A. A. Costa, J. G. F. Campos, and M. Copelli. Stochastic oscillations and dragon king avalanches in self-organized quasi-critical systems. *Scientific reports*, 9(1):3874, 2019.

33. O. Kinouchi and M. Copelli. Optimal dynamical range of excitable networks at criticality. *Nature physics*, 2(5):348–351, 2006.

34. O. Kinouchi, R. Pazzini, and M. Copelli. Mechanisms of self-organized quasicriticality in neuronal network models. *Frontiers in Physics*, 8:583213, 2020.

35. M. G. Kitzbichler, M. L. Smith, S. R. Christensen, and E. Bullmore. Broadband criticality of human brain network synchronization. *PLoS computational biology*, 5(3):e1000314, 2009.

36. M. A. Kramer, W. Truccolo, U. T. Eden, K. Q. Lepage, L. R. Hochberg, E. N. Eskandar, J. R. Madsen, J. W. Lee, A. Maheshwari, E. Halgren, et al. Human seizures self-terminate across spatial scales via a critical transition. *Proceedings of the National Academy of Sciences*, 109(51):21116–21121, 2012.

37. D. B. Larremore, W. L. Shew, and J. G. Restrepo. Predicting criticality and dynamic range in complex networks: effects of topology. *Physical review letters*, 106(5):058101, 2011.

38. X. Lei. Dragon-kings in rock fracturing: Insights gained from rock fracture tests in the laboratory. *The European Physical Journal Special Topics*, 205(1):217–230, 2012.

39. Y. Lin, K. Burghardt, M. Rohden, P.-A. Noël, and R. M. D'Souza. Self-organization of dragon king failures. *Physical Review E*, 98(2):022127, 2018.

40. K. Linkenkaer-Hansen, V. V. Nikouline, J. M. Palva, and R. J. Ilmoniemi. Long-range temporal correlations and scaling behavior in human brain oscillations. *Journal of Neuroscience*, 21(4):1370–1377, 2001.

41. V. S. L'vov, A. Pomyalov, and I. Procaccia. Outliers, extreme events, and multiscaling. *Physical Review E*, 63(5):056118, 2001.

42. Z. Ma, G. G. Turrigiano, R. Wessel, and K. B. Hengen. Cortical circuit dynamics are homeostatically tuned to criticality in vivo. *Neuron*, 104(4):655–664, 2019.

43. Z. F. Mainen and T. J. Sejnowski. Reliability of spike timing in neocortical neurons. *Science*, 268(5216):1503–1506, 1995.

44. D. Marković and C. Gros. Power laws and self-organized criticality in theory and nature. *Physics Reports*, 536(2):41–74, 2014.

45. P. Massobrio, L. de Arcangelis, V. Pasquale, H. J. Jensen, and D. Plenz. Criticality as a signature of healthy neural systems, 2015.

46. C. Meisel and C. Kuehn. Scaling effects and spatio-temporal multilevel dynamics in epileptic seizures. *PLoS One*, 7(2):e30371, 2012.

47. C. Meisel, E. Olbrich, O. Shriki, and P. Achermann. Fading signatures of critical brain dynamics during sustained wakefulness in humans. *Journal of Neuroscience*, 33(44):17363–17372, 2013.

48. C. Meisel, A. Storch, S. Hallmeyer-Elgner, E. Bullmore, and T. Gross. Failure of adaptive self-organized criticality during epileptic seizure attacks. *PLoS computational biology*, 8(1):e1002312, 2012.

49. G. Mikaberidze, A. Plaud, and R. M. D'Souza. Dragon kings in self-organized criticality systems. *Physical Review Research*, 5(4):L042013, 2023.

50. S. R. Miller, S. Yu, and D. Plenz. The scale-invariant, temporal profile of neuronal avalanches in relation to cortical γ–oscillations. *Scientific reports*, 9(1):16403, 2019.

51. G. Minadakis, E. Ventouras, S. D. Gatzonis, A. Siatouni, H. Tsekou, I. Kalatzis, D. E. Sakas, and J. Stonham. Dynamics of regional brain activity in epilepsy: a cross-disciplinary study on both intracranial and scalp-recorded epileptic seizures. *Journal of Neural Engineering*, 11(2):026012, 2014.

52. S. Monto, S. Vanhatalo, M. D. Holmes, and J. M. Palva. Epileptogenic neocortical networks are revealed by abnormal temporal dynamics in seizure-free subdural eeg. *Cerebral Cortex*, 17(6):1386–1393, 2007.

53. H. Nechad, A. Helmstetter, R. El Guerjouma, and D. Sornette. Andrade and critical time-to-failure laws in fiber-matrix composites: Experiments and model. *Journal of the Mechanics and Physics of Solids*, 53(5):1099–1127, 2005.

54. I. Osorio, M. G. Frei, D. Sornette, and J. Milton. Pharmaco-resistant seizures: self-triggering capacity, scale-free properties and predictability? *European Journal of Neuroscience*, 30(8):1554–1558, 2009.

55. I. Osorio, M. G. Frei, D. Sornette, J. Milton, and Y.-C. Lai. Epileptic seizures: quakes of the brain? *Physical Review E—Statistical, Nonlinear, and Soft Matter Physics*, 82(2):021919, 2010.

56. J. O'Byrne and K. Jerbi. How critical is brain criticality? *Trends in Neurosciences*, 45(11):820–837, 2022.

57. J. M. Palva and S. Palva. The correlation of the neuronal long-range temporal correlations, avalanche dynamics with the behavioral scaling laws and interindividual variability. *Criticality in Neural Systems*, pages 105–126, 2014.

58. L. Parish, G. Worrell, S. Cranstoun, S. Stead, P. Pennell, and B. Litt. Long-range temporal correlations in epileptogenic and non-epileptogenic human hippocampus. *Neuroscience*, 125(4):1069–1076, 2004.

59. R. Pazzini, O. Kinouchi, and A. A. Costa. Neuronal avalanches in watts-strogatz networks of stochastic spiking neurons. *Physical Review E*, 104(1):014137, 2021.

60. O. Peters, K. Christensen, and J. D. Neelin. Rainfall and dragon-kings. *The European Physical Journal Special Topics*, 205(1):147–158, 2012.

61. V. Pisarenko, A. Sornette, D. Sornette, and M. Rodkin. Characterization of the tail of the distribution of earthquake magnitudes by combining the gev and gpd descriptions of extreme value theory. *Pure and Applied Geophysics*, 171:1599–1624, 2014.

62. A. Ponce-Alvarez, A. Jouary, M. Privat, G. Deco, and G. Sumbre. Whole-brain neuronal activity displays crackling noise dynamics. *Neuron*, 100(6):1446–1459, 2018.

63. J. A. Roberts, K. K. Iyer, S. Finnigan, S. Vanhatalo, and M. Breakspear. Scale-free bursting in human cortex following hypoxia at birth. *Journal of Neuroscience*, 34(19):6557–6572, 2014.

64. M. Sachs, M. Yoder, D. Turcotte, J. Rundle, and B. Malamud. Black swans, power laws, and dragon-kings: Earthquakes, volcanic eruptions, landslides, wildfires, floods, and soc models. *The European Physical Journal Special Topics*, 205:167–182, 2012.

65. S. Scarpetta, I. Apicella, L. Minati, and A. De Candia. Hysteresis, neural avalanches, and critical behavior near a first-order transition of a spiking neural network. *Physical Review E*, 97(6):062305, 2018.

66. J. P. Sethna, K. A. Dahmen, and C. R. Myers. Crackling noise. *Nature*, 410(6825):242–250, 2001.

67. W. L. Shew, W. P. Clawson, J. Pobst, Y. Karimipanah, N. C. Wright, and R. Wessel. Adaptation to sensory input tunes visual cortex to criticality. *Nature Physics*, 11(8):659–663, 2015.

68. W. L. Shew and D. Plenz. The functional benefits of criticality in the cortex. *The neuroscientist*, 19(1):88–100, 2013.

69. O. Shriki, J. Alstott, F. Carver, T. Holroyd, R. N. Henson, M. L. Smith, R. Coppola, E. Bullmore, and D. Plenz. Neuronal avalanches in the resting meg of the human brain. *Journal of Neuroscience*, 33(16):7079–7090, 2013.

70. D. Sornette. Dragon-kings, black swans and the prediction of crises. *arXiv preprint arXiv:0907.4290*, 2009.

71. D. Sornette and G. Ouillon. Dragon-kings: mechanisms, statistical methods and empirical evidence. *The European Physical Journal Special Topics*, 205(1):1–26, 2012.

72. M. Süveges and A. Davison. A case study of a "dragon-king": The 1999 venezuelan catastrophe. *The European Physical Journal Special Topics*, 205(1):131–146, 2012.

73. C. Tetzlaff, S. Okujeni, U. Egert, F. Wörgötter, and M. Butz. Self-organized criticality in developing neuronal networks. *PLoS computational biology*, 6(12):e1001013, 2010.

74. D. Toker, I. Pappas, J. D. Lendner, J. Frohlich, D. M. Mateos, S. Muthukumaraswamy, R. Carhart-Harris, M. Paff, P. M. Vespa, M. M. Monti, et al. Consciousness is supported by near-critical slow cortical electrodynamics. *Proceedings of the National Academy of Sciences*, 119(7):e2024455119, 2022.

75. D. J. Watts and S. H. Strogatz. Collective dynamics of 'small-world'networks. *nature*, 393(6684):440–442, 1998.

76. J. Wilting and V. Priesemann. Between perfectly critical and fully irregular: a reverberating model captures and predicts cortical spike propagation. *Cerebral Cortex*, 29(6):2759–2770, 2019.

77. C. Witton, S. V. Sergeyev, E. G. Turitsyna, P. L. Furlong, S. Seri, M. Brookes, and S. K. Turitsyn. Rogue bioelectrical waves in the brain: the hurst exponent as a potential measure for presurgical mapping in epilepsy. *Journal of Neural Engineering*, 16(5):056019, 2019.

78. G. A. Worrell, S. D. Cranstoun, J. Echauz, and B. Litt. Evidence for self-organized criticality in human epileptic hippocampus. *Neuroreport*, 13(16):2017–2021, 2002.

79. J. Yan, Y. Wang, G. Ouyang, T. Yu, Y. Li, A. Sik, and X. Li. Analysis of electrocorticogram in epilepsy patients in terms of criticality. *Nonlinear Dynamics*, 83:1909–1917, 2016.

80. P. Zhao, X. Ding, L. Li, and G. Jiang. A review of cell-type specific circuit mechanisms underlying epilepsy. *Acta Epileptologica*, 6(1):18, 2024.

81. V. Zimmern. Why brain criticality is clinically relevant: a scoping review. *Frontiers in neural circuits*, 14:565335, 2020.